PAPER • OPEN ACCESS

Effect of tantalum on short-term creep of a 12%Cr-3%Co-0.07%Ta martensitic steel for steam blades

To cite this article: A E Fedoseeva *et al* 2020 *IOP Conf. Ser.: Mater. Sci. Eng.* **848** 012020

View the article online for updates and enhancements.

Recent citations

- Creep behavior and microstructure of a Ta-added 9%Cr steel with high B and low N contents
E Tkachev and A Belyakov

Effect of tantalum on short-term creep of a 12%Cr-3%Co-0.07%Ta martensitic steel for steam blades

A E Fedoseeva[1*], I S Nikitin[1], A E Fedoseev[1], E S Tkachev[1] and R O Kaibyshev[1]

[1]Belgorod National Research University, Pobeda 85 308015 Belgorod, Russia
[*] Corresponding author: fedoseeva@bsu.edu.ru

Abstract. 9-12%Cr martensitic steels are prospective materials for elements of boilers, tubes, pipes, heaters and steam blades for fossil power plants, which are able to work at ultra-supercritical parameters of steam. Decreasing N content and increasing B content together with increasing Cr content required the optimization of ferrite-stabilizing and austenite-stabilizing elements to avoid the formation of δ-ferrite at high temperatures. Addition of 3-4%Co, 0.01%B, 0.80%Cu and 0.07%Ta as austenite-stabilizing elements can compensate increasing Cr content up to 12% at decreasing N content to 0.003% and provides the δ-ferrite in the amount less than 10%. Two Co-containing 12%Cr steels were developed and investigated. The main difference between these steels is Ta addition; one of the 12%Cr steel studied contains 0.07%Ta, other 12%Cr steel is Ta-free one. Creep tests at 650°C and the applied stresses ranging 180-80 MPa with a step of 20 MPa for both Co-containing 12%Cr steels were carried out. Addition of Ta in the Co-containing 12%Cr steel provide the increment in the creep time to rupture at both high and low applied stresses. This increment in the creep properties due to Ta addition was explained by decrease in coarsening rate of Ta-rich MX carbonitrides during creep at 650°C.

1. Introduction

Nine to 12%Cr martensitic steels are prospective candidate as materials for elements of boilers, tubes, pipes, heaters and steam blades for new units of fossil power plants, which are able to work at ultra-supercritical parameters of steam [1-3]. High creep resistance of the 9-12%Cr martensitic steels is achieved by the formation of the tempered martensite lath structure (TMLS) after heat treatment consisted in normalizing and medium-temperature tempering [4-7]. The high-angle boundaries of prior austenite grains (PAGs), packets and blocks, as well as low-angle boundaries of martensitic laths are decorated by $M_{23}C_6$ carbides enriched by Cr, Fe and W [8,9], while fine MX carbonitrides play a role of the obstacles for rearrangements of free lattice dislocations into more stable configurations [10,11]. Main problem of 12%Cr steels with standard N content is the replacement of fine MX carbonitrides by coarse Z-phase during long-term thermal exposure that leads to appearance of creep strength breakdown and impede the prediction of long-term creep strength from short-term creep test data [12-15]. This replacement becomes possible due to the similar chemical compositions of MX carbonitrides and Z-phase (CrVN) particles [12]. In the steels with Cr content more than 9%, multiple acceleration of the Z-phase formation was fixed during creep [16]. Moreover, the mechanism of Z-phase nucleation are changed from nucleation of this phase on the MX/ferrite surface to direct transformation of face-centered cubic lattice of MX carbonitrides into tetragonal lattice of Z-phase. The last mechanism leads to the formation of coarse Z-phase particles with a mean size of 1 μm and full dissolution of fine MX carbonitrides; the steels loss the creep resistance after exposure of 10,000 h or more [16]. The addition

of Ta content in the steel can provide the three-fold separation of MX carbonitrides on V-rich MX, Nb-rich MX and Ta-rich MX and slows down the replacement of MX carbonitrides by coarse Z-phase.

The recent investigations showed that development of microstructural design of 9-10%Cr steel by optimization of austenite-stabilizing and ferrite-stabilizing elements allowed significantly increasing the creep time to rupture at 650°C [17-20]. Only low N content together with high B content could provide excellent 100,000 h creep strength of 110 MPa at 650°C using Larson-Miller parameter [17]. Increasing Cr content up to 12% for increasing in oxidation resistance together with low N and high B contents were compensated by the increasing in the content of austenite-stabilizing elements such as Co to 4% and Cu to 1%. New alloying schema allowed obtaining the δ-Fe content less than 10% (Fig. 1a,b). The increase in Co and B contents provides the slowing down of diffusion-controlled processes such as dislocation climb, particle coarsening according to Ostwald ripening and others [21-23]. The addition of Cu allows forming the nanoparticles with a size of 3-5 nm after tempering, which are nucleation sites for the fine Laves phase particles that provides narrow size distributions of last phase and retards the coarsening of this phase during thermal exposure [24,25]. Complex influence of alloying elements must provide improved creep resistance of 12%Cr steels. There are a lot of studies focused on investigation of the effect of Co, Cu and B on improved creep resistance [17-25]. However, effect of Ta on creep properties and microstructural changes in 9-12%Cr steel with low N and high B contents is not clear yet. The aim of the present study is to investigate the effect of Ta on creep properties of Co-containing 12%Cr steels.

2. Experimental procedure
The Ta-containing 12%Cr steel denoted here as 12%Cr-3Co-0.11(Ta+Nb) and Ta-free 12%Cr steel denoted here as 12%Cr-4Co-0.07Nb were prepared by vacuum induction melting as 100 kg ingots in Steel Institute (Institut für Eisenhüttenkunde (IEHK)), Aachen, Germany. Square bars with a 11 mm × 11 mm cross-section were cast and hot forged by the Joint Research Center, «Technology and Materials», Belgorod National Research University, Belgorod, Russia. Chemical compositions of the Co-containing 12%Cr steels with low N and high B contents are listed in Table 1.

Table 1. Chemical compositions of the Co-containing 12%Cr steels with low N and high B contents.

	C	Cr	Co	Mo	W	V	Cu	Nb	B	N	Ta
12%Cr-4Co-0.07Nb	0.09	11.3	3.9	0.63	2.4	0.24	0.78	0.07	0.009	0.003	-
12%Cr-3Co-0.11(Ta+Nb)	0.11	11.4	3.0	0.62	2.5	0.23	0.76	0.04	0.01	0.003	**0.07**

Both 12%Cr-4Co-0.07Nb and 12%Cr-3Co-0.11(Ta+Nb) steels were solution treated at 1050°C and 1070°C for 1 h, cooled in air, respectively, and subsequently tempered at 770°C for 3 h. Different normalizing temperature was chosen to provide the same PAG size for both steels. Flat specimens with a gage length of 25 mm and a cross section of 7 mm × 3 mm and cylindrical specimen with gauge length of 60 mm and a 6 mm diameter were crept until rupture at 650°C under the applied stresses of 180-80 MPa with a step of 20 MPa. The structural characterization was carried out using a transmission electron microscope JEOL–2100 (TEM) with an INCA energy dispersive X-ray spectrometer (EDS) on ruptured creep specimens. Identification of the precipitates was performed based of combination of EDS composition measurements of the metallic elements. The TEM specimens were prepared by electropolishing at room temperature using a solution of 10 pct perchloric acid in glacial acetic acid with Struers «Tenupol-5» machine. The precipitates were identified from both the chemical analysis and the selected-area diffraction method on at least 50 particles on the each portion. The volume fractions of the precipitated phases were calculated using the Thermo-Calc software with the TCFE7 database. The following phases were selected independently for calculation: BCC, FCC, M23C6 carbide, Laves phase (Fe2(W,Mo) (C14).

3. Results and Discussion

3.1 Microstructures after heat treatment

Microstructures of the Co-containing 12%Cr steels studied after heat treatment obtained by optical metallography and TEM are represented in Figure 1. Microstructural parameters after heat treatment for both steels are summarized in Table 2.
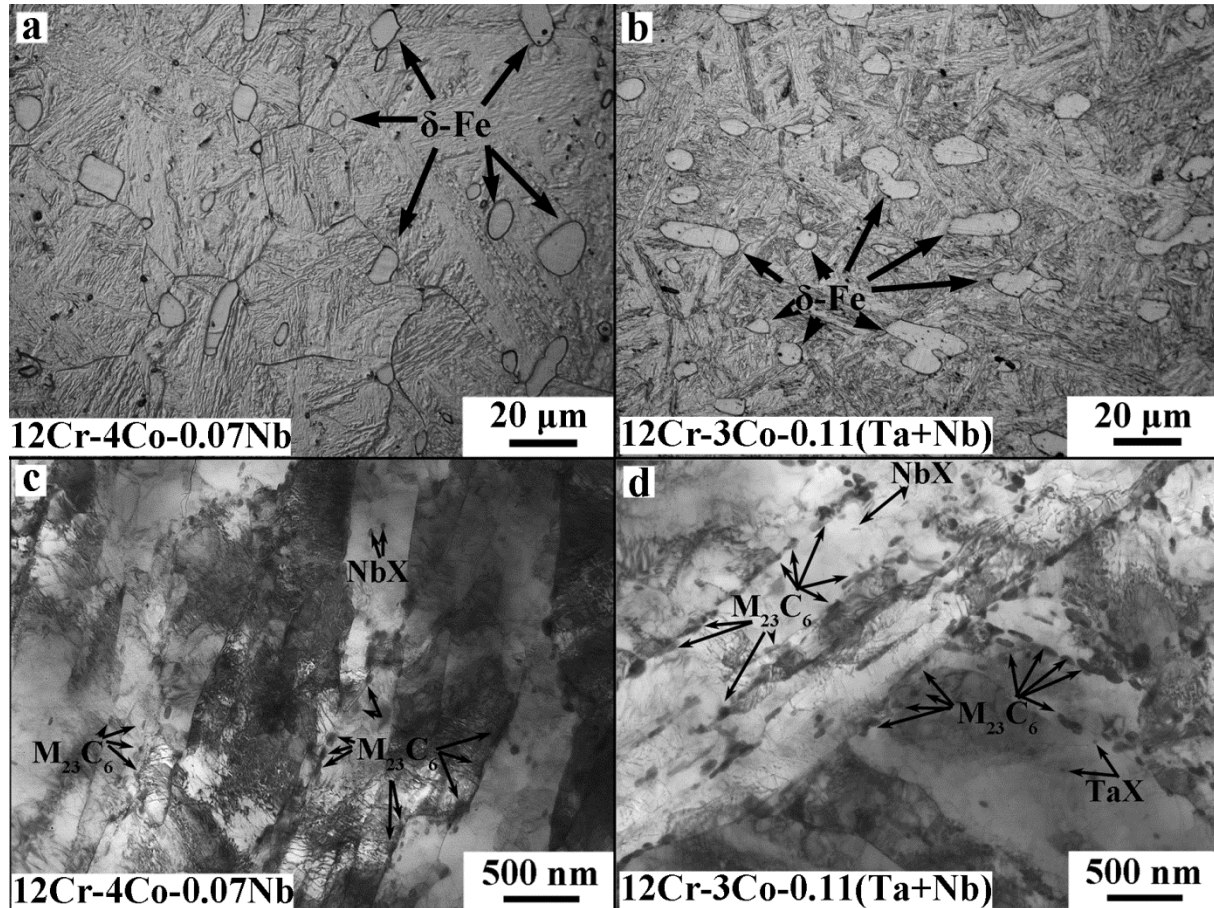

Figure 1. Microstructures of the 12%Cr-4Co-0.07Nb steel (a,c) and 12%Cr-3Co-0.11(Ta+Nb) steel studied (b,d) after normalizing at 1050-1070°C and tempering at 770°C obtained by optical metallography (a,b) and TEM of foils (c,d).

Table 2. Structural parameters of both 12%Cr steels studied after heat treatment.

	D_{PAG}, μm	Fraction of δ-Fe,%	d_{lath}, nm	Dislocation density, m^{-2}	Particle size, nm $M_{23}C_6$	MX	Particle fraction, % $M_{23}C_6$	MX
12Cr-4Co-0.07Nb	51±5	6±1	305±30	$(1.3±0.1)×10^{14}$	61±5	29±3	1.59	0.076
12Cr-3Co-0.11(Ta+Nb)	48±5	9±2	290±30	$(2.0±0.1)×10^{14}$	55±5	20±3	1.81	0.094

The PAG size was about 50 μm; fraction of δ was less than 10% for both steels after normalizing at 1050-1070°C (Figure 1a,b). After tempering at 770°C, the formation of tempered martensite lath structure (TMLS) was observed in both 12%Cr martensitic steels (Figure 1c,d). The transverse size of martensitic laths in both steels was nearly the same, whereas the dislocation density in the Ta-containing 12%Cr-3Co-0.11(Ta+Nb) steel is bigger than that in the Ta-free steel by a factor of 1.5 (Table 2). In both steels, Cr-rich $M_{23}C_6$ carbides decorated the high-angle PAG boundaries and low-angle boundaries of the martensitic laths (Figure 1c,d). The size of $M_{23}C_6$ carbides in both steels was

similar, while the fraction of these particles in the 12%Cr-3Co-0.11(Ta+Nb) steel is higher than that in the Ta-free steel (Table 2). The main difference between tempered structures of Ta-containing and Ta-free steels was MX carbonitrides. Two-phase separation of MX carbonitrides on Nb-rich MX and (Ta,Nb)-rich MX particles in the 12%Cr-3Co-0.11(Ta+Nb) steel was observed, whereas only Nb-rich MX phase was revealed in the 12%Cr-4Co-0.07Nb steel after tempering at 770°C.

The chemical composition of Nb-rich MX particles in the 12%Cr-3Co-0.11(Ta+Nb) steel was 4 wt.%Ti, 18%V, 30%Cr, 10%Fe and 38%Nb. The chemical composition of (Ta,Nb)-rich MX particles in the 12%Cr-3Co-0.11(Ta+Nb) steel was 2 wt.%V, 3%Cr+Fe, 10%Nb and 85%Ta. The chemical composition of Nb-rich MX particles in the 12%Cr-4Co-0.07Nb steel was 15 wt.%V, 16%Cr, 5%Fe and 64%Nb. The size of MX carbonitrides in the Ta-containing 12%Cr-3Co-0.11(Ta+Nb) steel is less than that in the Ta-free steel by a factor of 1.5, the fraction of MX carbonitrides in Ta-containing steel is higher than that of Ta-free steel (Table 2).

3.2 Creep properties

Figure 2 shows the creep rupture data of the steels at a temperature of 650°C. Times to rupture after creep tests for both steels are summarized in Table 3. For the 12%Cr-4Co-0.07Nb steel, creep tests at 650°C under the applied stresses ranging of 180-80 MPa with a step of 20 MPa are finished now, whereas for the 12%Cr-3Co-0.11(Ta+Nb) steel, creep tests at 650°C under the applied stresses of 180, 160 and 120 MPa is finished and creep tests at 650°C under the applied stresses of 140, 100 and 80 MPa are in progress.

Both steels demonstrated no any breakdowns on curves "Applied stress vs. Time to rupture" and "Minimal creep rate vs. Applied stress" (Figure 2).
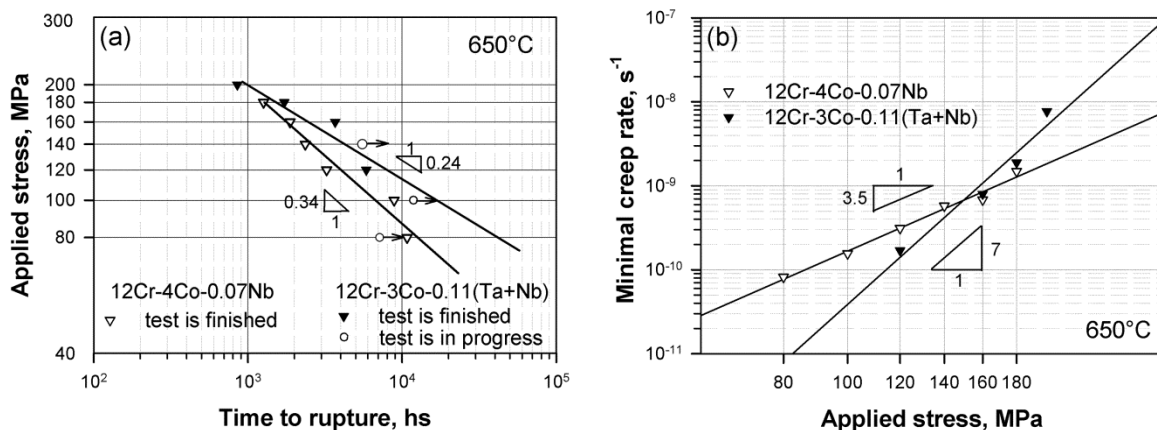

Figure 2. Time to rupture vs. stress curves (a) and the applied stress vs. minimal creep rate curves (b) demonstrate no evidence of any breakdowns for the both 12%Cr steels studied.

Table 3. Time to rupture in hours for creep tests used in the present study.

Applied stress, MPa	180 MPa	160 MPa	140 MPa	120 MPa	100 MPa	80 MPa
12Cr-4Co-0.07Nb	1263	1877	2355	3240	8875	10770
12Cr-3Co-0.11(Ta+Nb)	1721	3681	In process	5860	In process	In process

The 3%Co and 0.07%Ta additions significantly increased the creep strength under both the high and low applied stresses. Time to rupture in the Ta-containing steel was higher than that for Ta-free steel by a factor of 1.5-2.0 after at applied stresses of 180 MPa, 160 MPa and 120 MPa. Under the low applied stress (less 140 MPa), the effect of the Co and Ta additives on the creep strength did not tend to diminish in comparison with 9%Cr-3%Co steels, in which effect of Co decreased at the low applied stresses [6,20].

The experimental data obey a power law relationship throughout the whole range of the applied stress of the usual form [1,26,27]:

$$\dot{\varepsilon}_{\min} = A \times \sigma^n \exp\left(\frac{-Q}{RT}\right), \qquad (1),$$

where $\dot{\varepsilon}_{\min}$ is the minimum creep rate, σ is the applied stress, Q is the activation energy for a plastic deformation, R is the gas constant, T is the absolute temperature, A is a constant, and n is the "apparent" stress exponent. These plots provided the best linear fit with a regression coefficient of 0.98 for n=3.5 for the 12%Cr-4Co-0.07Nb steel and for n=7 for the 12%Cr-3Co-0.11(Ta+Nb) steel the whole applied stress interval. This n value at all tested stress regimes remains constant for both steels. This clearly indicates that there is no creep strength breakdown during the steady-state creep of the Co-containing 12%Cr martensitic steels [1,28]. The steady-state creep of the Co-containing 12%Cr steels was controlled using the same process for short- and long-term regions at a creep rate ranging from 10^{-6} to 10^{-11} s^{-1}. However, the mechanisms controlled steady-state creep for Ta-containing and Ta-free steel are different.

3.3 Crept microstructures
After high applied stress of 180 MPa, the microstructures of both Co-containing 12%Cr steels are similar with tempered state, TMLS remained (Figure 3a,b). The transverse lath size increased from about 300 nm to about 500 nm, while dislocation density did not change for both steels (Table 4). W-rich Laves phase particles precipitated along PAG and lath boundaries. The average size of Laves phase was 140 nm for both steels(Table 4). $M_{23}C_6$ carbides increased in size up to 90 nm in both steels, while the fraction of these particles in the Ta-containing steel is higher than that of the Ta-free steel (Table 4). No evidence for Z-phase particles was revealed in both steels. Nb-rich MX carbonitrides in the 12%Cr-4Co-0.07Nb steel and (Ta,Nb)-rich MX carbonitrides in the 12%Cr-3Co-0.11(Ta+Nb) steel increased their sizes to 30-35 nm. The main difference between steels was the fractions of secondary phase particles at 650°C (Table 4).

After low applied stress of 120 MPa, the microstructures of both steels strongly evolved. TMLS partially transformed into subgrain structure with a mean size of subgrains of 0.70 μm (Figure 3c,d, Table 5). Dislocation density in both steels decreased down to 10^{13} m^{-2}. This is accompanied with the coarsening of grain boundary $M_{23}C_6$ and Laves phase particles (Table 5). (Ta,Nb)-rich MX carbonitrides in the 12%Cr-3Co-0.11(Ta+Nb) steel retained their size of about 35-37 nm, whereas NbX carbonitrides in the 12%Cr-4Co-0.07Nb steel increased their size up to 45-50 nm (Table 5).

The precipitation of the MX carbonitrides on dislocations indicates that their coarsening rate is controlled by pipe diffusion. In this case, the continuous growth of the MX particles in both steels (Figure 4) should obey the following relationship:

$$d^n - d_0^{\,n} = K_p \tau, \qquad (2)$$

where d is subgrain/particle size at the time, d_0 is initial subgrain/particle size, K_p is constant of growth rate, τ is time, the coefficient n depends on the coarsening mechanism and is 5 that corresponds to pipe diffusion.
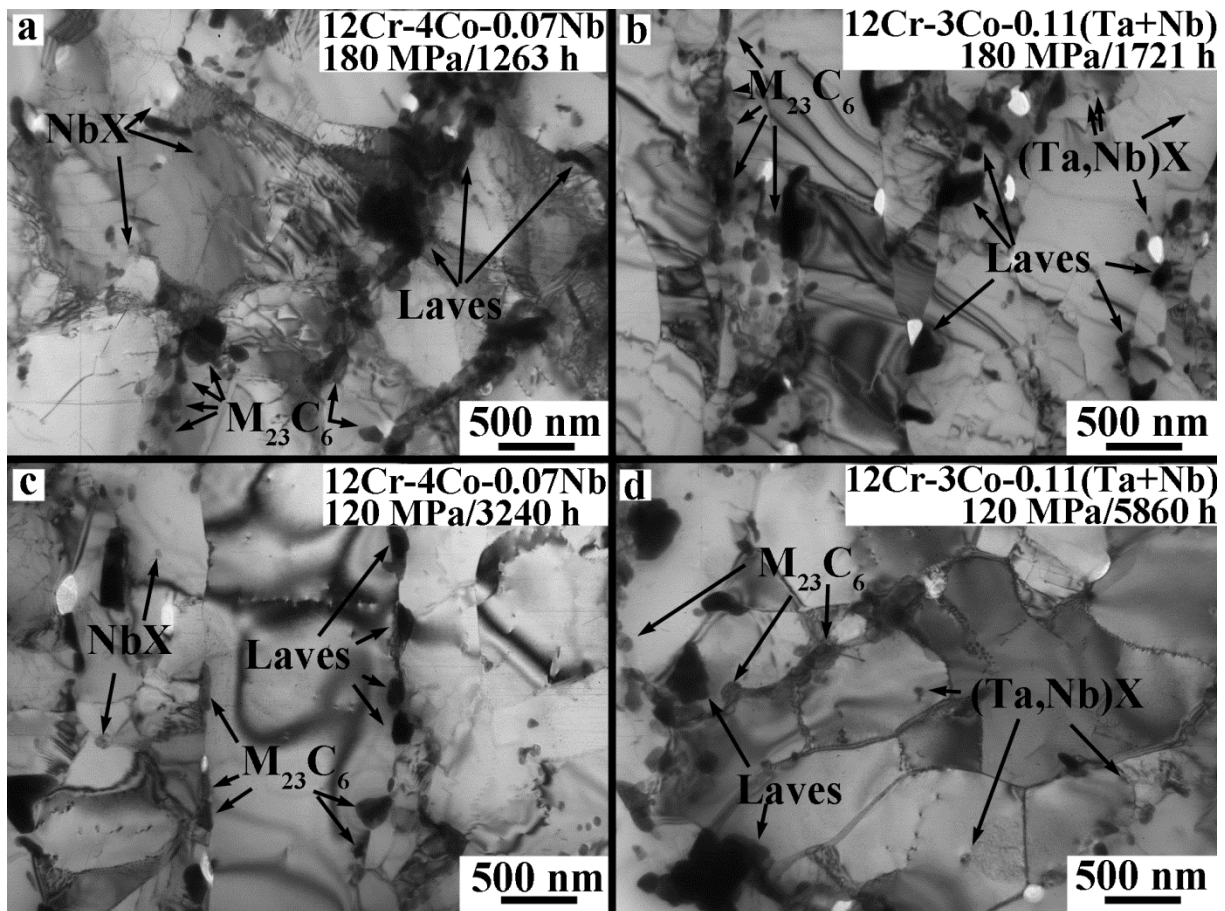
Figure 3. TEM images of microstructures of the 12%Cr-4Co-0.07Nb steel (a,c) and 12%Cr-3Co-0.11(Ta+Nb) steel studied (b,d) after creep tests at 650°C under the applied stresses of 180 MPa (a,b) and 120 MPa (c,d).

Table 4. Structural parameters of both 12%Cr steels studied after creep test at 650°C under an applied stress of 180 MPa.

	D_{PAG}, μm	Fraction of δ-Fe,%	d_{lath}, nm	Dislocation density, m^{-2}	Particle size, nm		Particle fraction, %	
					$M_{23}C_6$	MX	$M_{23}C_6$	MX
12Cr-4Co-0.07Nb	51±5	6±1	491±30	$(1.2±0.1)×10^{14}$	93±5	35±3	1.68	0.061
12Cr-3Co-0.11(Ta+Nb)	48±5	10±2	503±30	$(2.2±0.1)×10^{14}$	85±5	33±3	2.07	0.070

Table 5. Structural parameters of both 12%Cr steels studied after creep test at 650°C under an applied stress of 120 MPa.

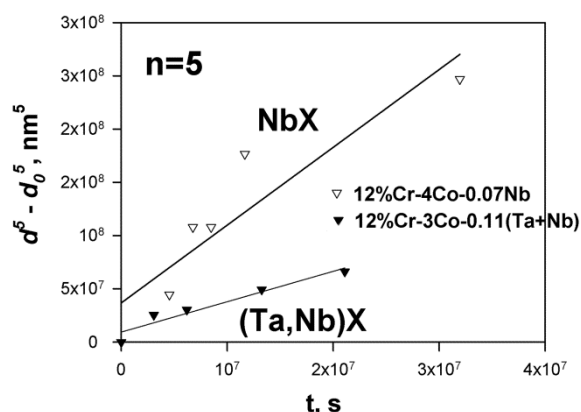|	D_{PAG}, μm	Fraction of δ-Fe,%	d_{lath}, nm	Dislocation density, m^{-2}	Particle size, nm		Particle fraction, %	
					$M_{23}C_6$	MX	$M_{23}C_6$	MX
12Cr-4Co-0.07Nb	51±5	6±1	730±50	$(0.8±0.1)×10^{14}$	109±5	45±3	1.68	0.061
12Cr-3Co-0.11(Ta+Nb)	48±5	10±2	650±50	$(0.7±0.1)×10^{14}$	96±5	37±3	2.07	0.070

Figure 4. The dependence of MX size on creep time at 650°C in the gage section for *n*=5 corresponding to pipe diffusion. NbX corresponds to 12%Cr-4%Co-0.07%Nb steel and (Ta,Nb)X corresponds to 12%Cr-3%Co-0.11%(Ta+Nb) steel.

According to Figure 4, constant of growth rate for NbX carbonitrides in the 12%Cr-4Co-0.07Nb steel was 7.31×10^{-45} $nm^5 s^{-1}$ with correlation coefficient of 0.85 for all experimental points after creep tests for ~10 000 h, whereas constant of growth rate for (Ta,Nb)X carbonitrides in the 12%Cr-3Co-0.07Nb steel was 2.85×10^{-45} $nm^5 s^{-1}$ with correlation coefficient of 0.93 for all experimental points after creep tests for ~6 000 h. So, addition of Ta in the Co-containing 12%Cr martensitic steels decreased coarsening rate by 61%. Slowing down of the coarsening of (Ta,Nb)-rich MX carbonitrides stabilizes TMLS during creep and can be one of the reasons for improved creep resistance of the Ta-containing 12%Cr steels.

4. Conclusions

New developed 12%Cr-(3-4%Co) steel with low N and high B contents demonstrated no evidence for any breakdowns on curves of "Time to rupture vs. Applied stress" and "Applied stress vs. minimal creep rate" due to absence of Z-phase particles, which replace the fine MX carbonitrides during creep testing. The addition of Ta in the 12%Cr steel together with decreasing in Co and Nb contents increased the creep time to rupture at 650°C. During creep (Ta,Nb)X particles demonstrated high thermal stability to the coarsening; the coarsening rate of these particles in the Ta-containing 12%Cr steel was twice less than NbX particles in the Ta-free 12%Cr-3Co-0.07Nb steel. The thermal stability of (Ta,Nb)X carbonitrides is one of the reasons for the increment in creep properties at 650°C.

References

[1]   Abe F, Kern T U, Viswanathan R 2008 *Creep resistant steels* (Cambridge: Woodhead Publishing in Materials) p 800
[2]   Kern T U, Staubli M, Scarlin B 2002 *ISIJ International* **42** 1515
[3]   Di Gianfrancesco A 2017 *Materials for Ultra-Supercritical and Advanced Ultra-Supercritical Power Plants* (Cambridge: Woodhead Publishing in Materials) p 900
[4]   Abe F 2007 *Int. J Press. Vess.Piping* **84** 3
[5]   Armaki H GH, Chen R P, Maruyama K, Igarashi M 2010 *Mater. Sci. Eng. A* **527** 6581
[6]   Fedoseeva A, Dudova N, Kaibyshev R 2017 *Phys. Met. Metall.* **118** 591
[7]   Mitsuhara M, Yamasaki Sh, Miake M, Nakashima H, Nishida M, Kusumoto J, Kanaya A 2016 *Phil. Mag. Lett.* **96** 76
[8]   Kostka A, Tak K G, Hellmig R J, Estrin Y, Eggeler G 2007 *Acta Mater.* **55** 539
[9]   Ghassemi-Armaki H, Chen R, Maruyama K, Igarashi M 2011 *Metall. Mater. Trans. A* **42** 3084

[10]   Fedoseeva A, Dudova N, Kaibyshev R 2016 *Trans. Indian Inst. Met.* **69** 211
[11]   Hald J 2016 *Trans. Indian Inst. Met.* **69** 183
[12]   Danielsen H K, Di Nunzio P E, Hald J 2013 *Metall. Mater. Trans. A* **44A** 2445
[13]   Strang A, Vodarek V 1996 *Mater. Sci. Technol.* **12** 552
[14]   Suzuki K, Kumai S, Kushima H, Kimura K, Abe F 2000 *Tetsu-to-Hagane* **86** 550
[15]   Suzuki K, Kumai S, Kushima H, Kimura K, Abe F 2003 *Tetsu-to-Hagane* **89** 691
[16]   Danielsen H K 2016 *Mat. Sci. Technol.* **32** 126
[17]   Dudova N, Mishnev R, Kaibyshev R 2019 *Mater. Sci. Eng. A* **766** 138353
[18]   Fedoseeva A, Kozlov P, Dudko V, Skorobogatykh V, Shchenkova I, Kaibyshev R 2015 *Phys. Met. Metall.* **116** 1047
[19]   Dudko V, Fedoseeva A, Belyakov A, Kaibyshev R 2015 *Phys. Met. Metall.* **116** 1165
[20]   Fedoseeva A, Dudova N, Kaibyshev R, Belyakov A 2017 *Metals* **7** 573
[21]   Abe F 2011 *Procedia Engineering* **10** 94
[22]   Helis L, Toda Y, Hara T, Miyazaki H, Abe F 2009 *Mater. Sci. Eng. A* **510–511** 88
[23]   Kipelova A, Odnobokova M, Belyakov A, Kaibyshev R 2013 *Metall. Mater. Trans. A* **44** 577
[24]   Klueh R L 2005 *International Materials Reviews* **50** 287
[25]   Futamura Yu, Tsuchiyama T, Takaki S 2001 *ISIJ International* **41** S106
[26]   Cadek J 1994 *Creep in Metallic Materials* (Prague: Academia) p 372
[27]   Kassner M E, Pérez-Prado M T 2004 *Fundamentals of creep in metals and alloys* 1st ed (New York: Elsevier Science) p 288
[28]   Abe F 2015 *Metall. Mater. Trans. A* **46** 5610